EXAFS and *ab Initio* Molecular Orbital Studies on the Structure of Solvated Silver(I) Ions

Yuko Tsutsui,[1a] Ken-ichi Sugimoto,[1a] Hiroaki Wasada,[1b] Yasuhiro Inada,[1a] and Shigenobu Funahashi*,[1a]

Laboratory of Analytical Chemistry, Faculty of Science, Nagoya University, Chikusa, Nagoya 464-01, Japan, and Department of Chemistry, Faculty of General Education, Gifu University, 1-1 Yanagido, Gifu 501-11, Japan

Received: November 13, 1996; In Final Form: February 3, 1997[⊗]

Structure parameters of solvated silver(I) ions in eight neat solvents were determined by extended X-ray absorption fine structure spectroscopy. The coordination geometry of the solvated silver(I) ion is four-coordinate tetrahedral at the Ag−O bond distances of 239 pm in trimethylphosphate, 239 pm in *N*,*N*-dimethylformamide, 238 pm in 1,1,3,3-tetramethylurea, and 238 pm in dimethyl sulfoxide as oxygen-donating solvents, and at the Ag−N bond distances of 229 pm in acetonitrile, 230 pm in 2-methylpyridine, 229 pm in *n*-propylamine, and 231 pm in ethylenediamine as nitrogen-donating solvents. According to our present *ab initio* molecular orbital calculations concerning the structure of the silver(I) ion bound by n molecules of hydrogen cyanide ($n = 1-6$) and acetonitrile ($n = 1-5$) in the gas phase, the maximal stabilization for the solvation is observed at $n = 4$. The results of the theoretical calculations in the gas phase are consistent with the experimental observations in solution.

Introduction

A variety of coordination geometries have been observed around the Ag(I) ion in both solid and liquid phases. It has been shown that the Ag(I) ion forms four-coordinate tetrahedral complexes with acetonitrile,[2] pyridine,[3,4] and bipyridine derivatives such as 4,4′,6,6′-tetramethyl-2,2′-bipyridine[5] in the solid state. On the other hand, the structures of two-coordinate linear Ag(I) complexes with ammonia,[6] imidazole,[7] and pyridine[4] have been determined by X-ray crystallography. Interestingly, for the pyridine complexes, the single-crystal structures with both the linear and tetrahedral geometries were observed in the same crystal.[4] In solution, two-, three-, or four-coordinate Ag(I) complexes were observed in response to the mole ratio of the ligand to the Ag(I) ion for ammonia,[8] pyrazine,[9] and bidentate Schiff base derivatives.[10,11] However, the solvation structures around the Ag(I) ion in neat solvents have not been observed without four-coordinate tetrahedral geometry. It has been demonstrated that the Ag(I) ion is tetrahedrally solvated by four solvent molecules in water,[12−16] liquid ammonia,[16] pyridine,[16,17] and acetonitrile[16,18] using the X-ray absorption,[12,16] neutron diffraction,[13] and X-ray diffraction techniques.[14,15,17,18]

The hydration structure of the first-row transition metal(II) ions is six-coordinated octahedral, whereas in a bulky solvent the solvation number of their metal(II) ions changes from 4 or 5 corresponding to the metal ion size and/or the bulkiness of solvent molecules.[19] Though the effective ionic radius of the Ag(I) ion is certainly larger than those of first-row transition metal(II) ions,[20] the fact that the Ag(I) ion in water has a four-coordinate structure is interesting. This suggests that the solvation number is affected by the electronic properties and the size of the Ag(I) ion. In order to elucidate these factors, we observed the solvation structures of the Ag(I) ion in eight solvents with the oxygen or nitrogen as a donor atom by the extended X-ray absorption fine structure (EXAFS) method. We selected water, trimethylphosphate (TMP), *N*,*N*-dimethylformamide (DMF), 1,1,3,3-tetramethylurea (TMU), and dimethyl sulfoxide (DMSO) as the oxygen-donating solvents, and acetonitrile (CH_3CN), *n*-propylamine (PA), ethylenediamine (EN), pyridine (PY), and 2-methylpyridine (2-MePY) as the nitrogen-donating solvents. Furthermore, to obtain the systematic characterizations of the structural and electronic properties of the fanciful species with the coordination number from 1 to 6, the theoretical *ab initio* molecular orbital calculations were performed on the structures of the Ag(I) ion with hydrogen cyanide and acetonitrile in the gas phase.

Experimental and Computational Section

Preparation of Sample Solutions. TMP, DMF, TMU, and DMSO were dried over 4A molecular sieves and then distilled under reduced pressure. Acetonitrile was distilled after refluxing for 2 h in the presence of P_2O_5 (2 g/dm^3). EN was purified as described in the literature.[21] PA was distilled after being dried over zinc powder. PY and 2-MePY were distilled after dehydration using BaO. Sample solutions were prepared by dissolving a weighted amount of silver(I) salts ($AgNO_3$, $AgCF_3SO_3$, and $AgClO_4$) in each purified solvent under the nitrogen atmosphere. All chemicals used were of reagent grade (Wako Pure Chemical Industries, Ltd., Japan).

EXAFS Measurements and Data Reduction. Silver K-edge X-ray absorption data were collected in the transmission mode at ambient temperature using the BL10B station at the Photon Factory of the National Laboratory for High Energy Physics.[22,23] Monochromatized X-rays were obtained using an Si(311) channel-cut crystal. The incident and transmitted X-ray intensities were simultaneously measured by the ionization chambers filled with Ar and Kr gas, respectively. Sample solutions for the EXAFS measurements were sealed in a cell with windows of boron nitride plates and an adjustable 4−7 mm path length.

Details of the data reduction of the raw EXAFS spectra have been previously described.[19] The threshold energy of a K-shell electron, E_0, was selected as the position of the half-height of the edge jump in each sample. The observed EXAFS oscillation ($\chi_{obsd}(k)$) extracted from the raw EXAFS spectrum was weighted by k^3, and its Fourier transformation was performed. The main peak in the Fourier transform was extracted and made into an inverse Fourier transformation to obtain the Fourier-filtered $k^3\chi(k)$ values. In order to determine the structure parameters, the model $\chi(k)$ function was fitted to the Fourier-filtered $k^3\chi(k)$ values over the k range from 2.0×10^{-2} to 10.5×10^{-2} pm^{-1}.

[⊗] Abstract published in *Advance ACS Abstracts,* March 15, 1997.

S1089-5639(96)03792-9 CCC: $14.00

The model function is given by the single-electron excitation and single-scattering theory (eq 1)[24−27]

$$\chi(k) = \frac{n}{kR^2} \exp\left(-2\sigma^2k^2 - \frac{2R}{\lambda}\right) F(\pi,k) \sin(2kR - \alpha(k)) \quad (1)$$

where $F(\pi,k)$ is the backscattering amplitude from the scatterer, R is the distance from the absorbing atom to the scatterer, n is the number of the scatterer, σ is the Debye−Waller factor, λ is the mean free path of the photoelectron, and $\alpha(k)$ is the total scattering phase shift. For the determination of the structure parameters of structurally unknown samples, the values of $F(\pi,k)$ and $\alpha(k)$, when the Ag(I) ion was surrounded by oxygen and nitrogen donor atoms, were determined using the Fourier-filtered $k^3\chi(k)$ curves of H_2O and PY solutions of $AgNO_3$, respectively. In these solvents, the solvation structures were previously determined.[12−15,17,18] In this procedure, firstly, the values of λ (322 pm for H_2O and 293 pm for PY) and σ (12.0 pm for H_2O and 10.7 pm for PY) were estimated by using the literature values of $F(\pi,k)$ and $\alpha(k)$ reported by McKale *et al*.[28] with the values of n and R fixed for each sample (4.0 and 241 pm for H_2O and 4.0 and 230 pm for PY). Secondly, the $F(\pi,k)$ and $\alpha(k)$ values were refined by fixing the values of n, R, σ, and λ for each sample. Then, using these refined $F(\pi,k)$ and $\alpha(k)$ values, n, R, and σ were optimized as variables for the other unknown samples. The values of E_0 were kept constant in all calculations.

Computational Details. We considered the solvation reactions of the silver(I) cation with hydrogen cyanide (reaction 2) and acetonitrile (reaction 3) in order to estimate the characterizations of the structural and electronic properties for solvation of the Ag(I) ion.

$$Ag^+ + nHCN \rightarrow [Ag(NCH)_n]^+ \quad (2)$$

$$Ag^+ + nCH_3CN \rightarrow [Ag(NCCH_3)_n]^+ \quad (3)$$

Structures of $[Ag(solvent)_n]^+$ (solvent HCN, $n = 1-6$; solvent CH_3CN, $n = 1-5$) were fully optimized at the restricted Hartree−Fock (RHF) level. As the basis sets we used Huzinaga's MIDI.[29] In the case of HCN, two polarization p functions were added to the Ag basis set and a polarization d function was added to each of the carbon and nitrogen basis sets; the exponents are 0.105 and 0.035 for silver, 0.600 for carbon, and 0.864 for nitrogen. The final basis sets are [433321/432111/421] for Ag, [421/31/1] for C and N, and [31] for H. In the case of CH_3CN, the same basis sets as used for the HCN-solvated silver(I) ions were used except for the methyl group of CH_3CN. Huzinaga's MINI basis sets contracted to [43/4] for C and [4] for H were placed on the methyl groups.[29] The vibrational partition functions concerning the internal rotational modes of the methyl group were replaced with the partition functions of its internal rotation.

The electronic stabilization energy (ΔE_{solv}) by solvation according to reactions 2 and 3 is given by eq 4

$$\Delta E_{solv} = E_{Ag(solvent)^{n+}} - (E_{Ag^+} + nE_{solvent}) + \Delta E_{BSSE} \quad (4)$$

where $E_{solvent}$, E_{Ag^+}, and $E_{Ag(solvent)^{n+}}$ are energies of the free solvent, silver cation, and solvated silver(I) ion with the solvation number of n, respectively. The basis set superposition errors (BSSE) between the Ag(I) ion and solvent molecules were estimated by the Boys−Bernardi counterpoise method.[30,31] Stabilization energies described with the standard Gibbs free energy (ΔE_{solv}) at 1 atm and 25.0 °C were computed using the partition functions in order to take into account the thermal effect.[32]

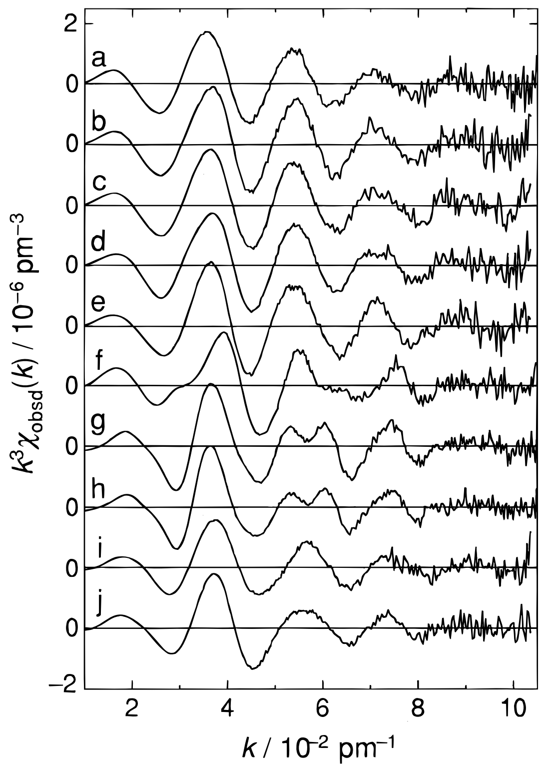

Figure 1. Observed EXAFS oscillations weighted by k^3 for $AgNO_3$ in 10 neat solvents: (a) water, (b) TMP, (c) DMF, (d) TMU, (e) DMSO, (f) CH_3CN, (g) PY, (h) 2-MePY, (i) PA, (j) EN.

We also considered the two model reactions 5 and 6 for the comparison of the stabilization energies between the tetra- and pentasolvated Ag(I) species. All five HCN molecules are in

$$Ag^+ + 5HCN \rightarrow [Ag(NCH)_5]^+ \quad (5)$$

$$Ag^+ + 5HCN \rightarrow [Ag(NCH)_4]^+HCN \quad (6)$$

the first-coordination sphere in the product of reaction 5, while the product according to reaction 6 has four HCN molecules in the first coordination sphere and one HCN in the outer coordination sphere.[33]

We used the Gaussian 92 program[34] on IBM RS6000 for all the *ab initio* molecular orbital calculations and the MOLCAT program[35] on a Macintosh computer to visualize the vibrational modes.

Results and Discussion

Solvation Structures of Ag(I) Ions in Several Solvents As Determined by EXAFS. The observed k^3-weighted EXAFS oscillations ($k^3\chi_{obsd}(k)$) of Ag(I) ions in 10 solvents are shown in Figure 1. Their corresponding Fourier transforms, uncorrected for the phase shift, are shown in Figure 2. The Fourier-filtered $k^3\chi(k)$ values and the calculated $k^3\chi(k)$ curves depicted using the obtained structure parameters are shown by the circles and by the solid lines, respectively, in Figure 3 for the unknown eight samples.

The obtained structure parameters are listed in Table 1 together with the reported values for the H_2O, CH_3CN, and PY solutions. The solvation number of the silver(I) ion is four in all solvents studied in this work. According to the review of crystallographic data for Ag(I) compounds,[14] the mean values

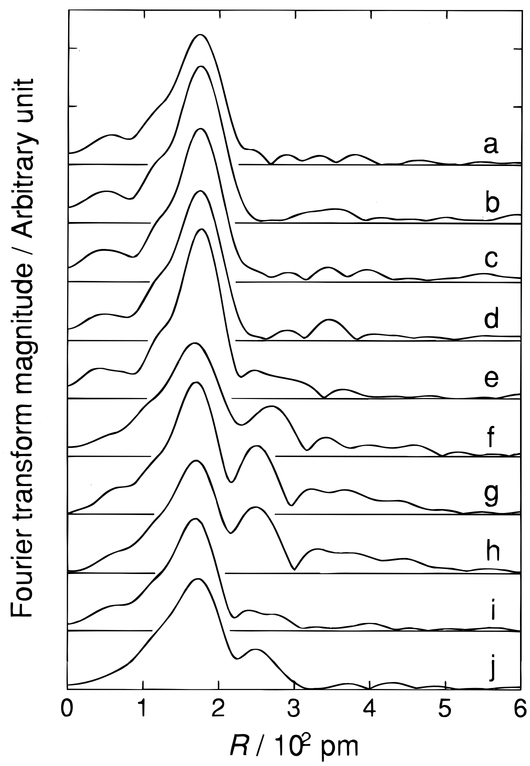

Figure 2. Fourier transforms of the $k^3\chi_{obsd}(k)$ curves shown in Figure 1, uncorrected for the phase shift: (a) water, (b) TMP, (c) DMF, (d) TMU, (e) DMSO, (f) CH_3CN, (g) PY, (h) 2-MePY, (i) PA, (j) EN.

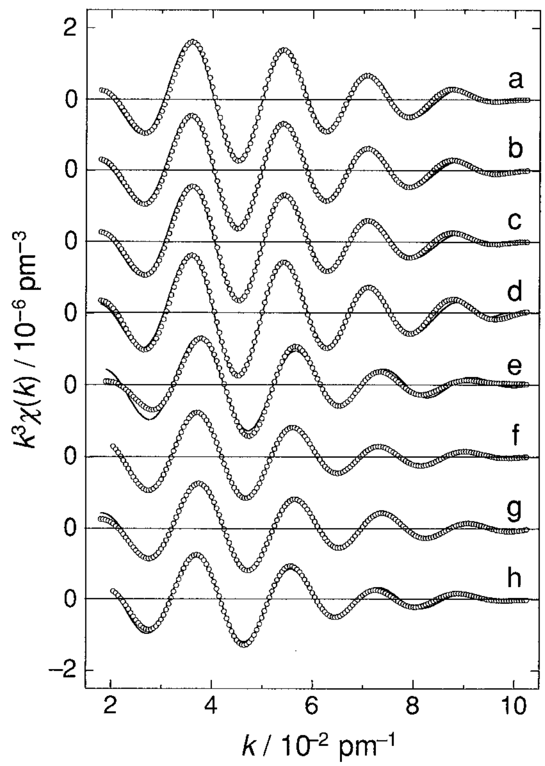

Figure 3. Fourier-filtered $k^3\chi(k)$ values (circles) and calculation curves (solid lines) depicted using the parameters in Table 1 for eight sample solutions: (a) TMP, (b) DMF, (c) TMU, (d) DMSO, (e) PY, (f) 2-MePY, (g) PA, (h) EN.

of Ag−O distances are 213, 240, and 250 pm for two-coordinate linear, four-coordinate tetrahedral, and six-coordinate octahedral geometry, respectively. The determined Ag−O distances for the oxygen-donating solvents, TMP, DMF, TMU, and DMSO, are very similar to that for the four-coordinate tetrahedral

TABLE 1: Structure Parameters of Ag(I) Ions in Various Solvents[a]

solvent	C_{Ag}/mol kg^{-1}	n[b]	R/pm[c]	σ/pm[d]
H_2O	0.303	4[e]	241[e]	12.0(0.1)
H_2O[f]		4.0	238−243	
TMP	0.273	4.0(0.1)	239(1)	10.8(0.2)
DMF	0.308	3.9(0.1)	239(1)	10.9(0.1)
TMU	0.318	3.9(0.1)	238(1)	11.2(0.1)
DMSO	0.283	3.9(0.1)	238(1)	10.2(0.1)
PY	0.490	4[e]	230[e]	10.7(0.1)
PY[g]		4.0	230	
PY[h]		3.9	229	
PY[i]		4	232	
CH_3CN	0.399	3.7(0.2)	229(1)	10.6(0.2)
CH_3CN[j]		4.0	225	
CH_3CN[h]		3.7	224	
CH_3CN[k]		4	218−233	
2-MePY	0.517	3.9(0.1)	230(1)	12.2(0.1)
PA	0.367	3.8(0.1)	229(1)	11.1(0.1)
EN	0.364	4.1(0.2)	231(1)	12.0(0.2)

[a] The values obtained in this study are the results for $AgNO_3$. The values of E_0 were within 25.50 ± 0.01 keV for all samples. [b] Coordination number. [c] Interatomic distance. [d] Debye−Waller factor. [e] Fixed values (see in text). [f] Determined by the X-ray and the neutron diffraction methods. References 12−15. [g] Determined by the X-ray diffraction method. Reference 17. [h] Determined by the EXAFS method. Reference 16. [i] Values observed in the single crystal. Reference 3. [j] Determined by the X-ray diffraction method. Reference 18. [k] Values observed in the single crystal. Reference 2.

structure. The geometrical structure of the Ag(I) ion in PY and AN has been determined to be four-coordinate tetrahedral using X-ray diffraction.[17,18] The obtained Ag−N bond lengths are 230 pm in 2-MePY, 229 pm in PA, and 231 pm in EN, which are in agreement with that in PY. This indicates that there is tetrahedral solvation of the Ag(I) ion in these solvents.

We must note here that the contact ion-pair formation of the Ag(I) ion with its counteranion was reported in the previous works at the higher concentrations of the Ag(I) salts in the X-ray diffraction experiments.[14] Some 100 mM concentrations of samples used in the present study are relatively lower than those in the previous diffraction experiments, and then the contact ion-pair formation might be negligible under our experimental conditions judging from available ion-pair formation constant data in water.[36] In the case of the oxygen-donating solvents, the distinction whether the oxygen atom bound to the Ag(I) ion comes from the solvent or from the counteranion was impossible. And then, in addition to the salt of $AgNO_3$, we have carried out the EXAFS measurements for $AgCF_3SO_3$ and $AgClO_4$ in water and $AgCF_3SO_3$ in TMP with the lowest dielectric constant (ϵ = 16.4) among the oxygen-donating solvents used in this study. The obtained structure parameters, n, R/pm, and σ/pm, were respectively as follows: for $AgCF_3SO_3$ in water, 4.0 ± 0.1, 241 ± 1, and 12.3 ± 0.1, for $AgClO_4$ in water, 3.9 ± 0.1, 240 ± 1, and 14.3 ± 0.2, and for $AgCF_3SO_3$ in TMP, 4.1 ± 0.1, 239 ± 1, and 11.2 ± 0.2. These values are perfectly consistent with those for $AgNO_3$ as shown in Table 1, and also there is no difference in the $k^3\chi_{obsd}(k)$ curves and Fourier transforms. Therefore, the Ag(I) ion does not form the contact ion-pair under our experimental conditions, and all the surrounding molecules around the Ag(I) ion are the solvents. In the case of the nitrogen-donating solvents, the unsymmetrical behavior will be observed in the EXAFS oscillations by the participation of a counteranion into the first-coordination sphere of the Ag(I) ion, because the Ag−O interactions should have a large difference in the bond length from the Ag−N interactions. Because there was no such behavior as shown in Figure 1, we concluded that the contact ion-pair also is not formed in the nitrogen-donating solvents.

Dimethyl sulfoxide can coordinate to metal ions via either its oxygen or sulfur atom. Usually, soft metal ions prefer to bind to DMSO molecules at the sulfur site, while harder metal ions bind to them at the oxygen site. Although this trend is observed in general, there are a variety of cases where the coordinated DMSO molecules are bound to Pt(II),[37] Pd(II),[38] and Rh(III) ions[39] via the sulfur atom, to Hg(II)[40] and Cd(II)[41] ions via the oxygen atom, and to Pt(II)[42] and Ru(II)[43] ions via both the oxygen and sulfur atoms. As is apparent from Figure 1, the EXAFS oscillation for the Ag(I) ion in DMSO is very similar to those in the other solvents with the donor atom of oxygen. This strongly suggests that all the DMSO molecules are coordinated to the Ag(I) ion through their oxygen atoms. Furthermore, the interaction peak in the second-coordination sphere in DMSO, observed around 250 pm in Figure 2, is slightly larger than those for the other oxygen-donating solvents. The peak can be assigned to the interactions between the Ag(I) ion and the heavier sulfur atom of DMSO. Therefore, we analyzed the EXAFS oscillation in DMSO using the single-shell model composed by the oxygen atoms and determined that the first-coordination sphere contains four oxygen atoms at the Ag−O bond length of 238 ± 1 pm. This is also confirmed by the fact that the Ag−O bond distance for DMSO is almost the same as those for the oxygen-donating solvents (vide supra).

Previously, we have indicated the variation in coordination number that the solvation structures in TMU are square pyramidal for the Mn(II) and Ni(II) ions, distorted tetrahedral for the Co(II) and Cu(II) ions, tetrahedral for the Zn(II) ion, and octahedral for the Cd(II) and In(III) ions, while in water, all these metal ions are six-coordinated octahedrons.[19] It has been concluded that the coordination number of the solvated metal ions in nonaqueous solvents is mainly determined by the bulkiness of solvent molecules and the size of central metal ions, although the ligand field stabilization energy is added as a perturbation for the determination.[19] However, in the case of the Ag(I) ion of a relatively large size, since the coordination number is 4 in the smaller solvents such as H_2O, DMSO, CH_3CN, and DMF as well as in TMU, the coordination number of 4 should be due to the lower charge of the silver(I) ion (vide infra).

It should be noticed that peaks at $R = 200-300$ pm in Figure 2 for CH_3CN, PY, 2-MePY, and EN correspond to the existence of the longer interaction shell. In the case of PY and 2-MePY, this is characteristic of the Ag···C nonbonding interactions. The appearance of these peaks suggests that the pyridine skeleton is arranged to the Ag(I) ion with the Ag−N−C angle of 120° as observed in the crystal.[3,4] In the case of CH_3CN, the peaks are thought to be due to the nonbonding Ag···C interactions and their multiple scattering. In the crystal phase, the linear CH_3CN molecules are arranged to the Ag(I) center with the Ag−N−C angles of *ca*. 180°.[2] There is a possibility of the bent orientation of CH_3CN molecules to the electron-rich Ag(I) ion as previously indicated for the Cu(I) and Ag(I) ions in acetonitrile[44] because of the strong π-accepting ability of CH_3CN molecules. However, we have concluded that the CH_3CN molecules are coordinated to the Ag(I) ion with the linear Ag−N−C angle, because the main contribution to the solvation energy must come from the σ-bond of the donating atoms of the coordinated solvent molecules. The σ-interaction has the best advantage of the linear orientation of CH_3CN to the Ag(I) ion. The peak intensity for the Ag···C interactions observed at around 270 pm for CH_3CN relative to the first-coordination peak is lower than those observed for PY and 2-MePY, as is shown in Figure 2. However, in the case of the Cu(I) and Cu(II) ions, the opposite trend is observed.[44] Since the Ag−N bond length is longer than that of the Cu−N bond, the Ag···C distance should be more elongated in the case of the linearly coordinating linear solvent of CH_3CN rather than in the case of PY and 2-MePY, in which the Ag−N−C angle is 120°. Therefore, the trend of the observed peak ratio can also be explained by the postulation that the Ag−N−C angle is 180° for CH_3CN.

As apparent from Figure 2, the intense peak at *ca*. 250 pm due to the Ag···C nonbonding interaction is observed in EN while the corresponding peak is not distinct in PA, which coordinates to the Ag(I) ion only in the monodentate mode. Therefore, an EN molecule bound to the Ag(I) ion forms a chelate ring in neat EN. Two EN molecules then are coordinated to an Ag(I) ion as a bidentate ligand, as observed for the Cu(II)−EN complexes in EN and water.[45] The Ag−N bond length of 231 pm for $[Ag(en)_2]^+$ is in accord with those of 233−235 pm of $[Ag(L)_2]^+$, where L is a Schiff base derivative[10] having the same chelate skeleton as EN. In addition, it is interesting that the crystal structure of the Ag(I)−EN complex was previously determined to be two-coordinate linear,[46] in which the EN molecule acts as a monodentate bridging ligand.

There is an alternative way to use the CH_3CN solution as a standard for the EXAFS analysis of the solvation structure in nitrogen-donating solvents instead of the PY solution. However, because the four Ag−N bonds in the single crystal of $Ag(CH_3CN)_4{}^+$ differ in length largely (218−233 pm)[2] as compared with $Ag(py)_4{}^+$,[3] we used the PY solution as the standard sample in this study. The obtained Ag−N bond length of 229 pm in CH_3CN seems to be slightly longer than the reported values.[16,18] The bond lengths in aliphatic amine, PA and EN, are comparable to that in liquid ammonia (231 pm).[16] The fact that the Ag−N bond distance is only 2 pm longer in EN than in PA supports that there is no significant chelate strain on the chelate ring of the EN molecules coordinated to the large Ag(I) ion because of the d^{10} configuration of the Ag(I) ion.

Judging from the free energy of transfer of the Ag(I) ion in several solvents,[47] the Ag(I) ion is more strongly solvated in PY than in CH_3CN. However, the Ag−N bond distance is slightly shorter in AN than in PY. Because the electron cloud of molecular orbitals contributing to the σ-bonding of the Ag(I) ion with the nitrogen atom of CH_3CN should be less expanded in comparison with that of PY, the CH_3CN molecules can approach closer to the central Ag(I) ion in spite of weaker bonding.

A comparison of the structure parameters in PY and 2-MePY shows that a methyl group at the 2-position of the pyridine skeleton does not sterically affect the solvation structure of the Ag(I) ion. Thus the first-coordination sphere seems to have enough space to accommodate the methyl substitutes around the tetrahedrally solvated Ag(I) ion.

On $[Ag^I(L)_2]$, where L is 8-hydroxyquinoline (L_1)[48] or 2-pyridinecarboxylate (L_2),[49] which has both oxygen and nitrogen as a donor atom, the Ag−N bond length (av. 215.0 pm for L_1, 220.7 pm for L_2) is shorter than the Ag−O distance (av. 247.8 pm for L_1, 252.4 pm for L_2). This is consistent with the fact that the Ag−O distance is longer than the Ag−N one in the present solvated silver(I) ions.

Theoretical Calculations: Solvation Structure and Coordination Number of the Ag(I) Ion Bound by HCN and CH_3CN. In Table 2 are given the optimized structures of the HCN-solvated Ag(I) ions, $[Ag(NCH)_n]^+$ ($n = 1-6$) and the CH_3CN-solvated Ag(I) ions, $[Ag(NCCH_3)_n]^+$ ($n = 1-5$) with the corresponding symmetries together with the total energy and the Mulliken charge on the silver atom. The vibrational analysis has confirmed that all the obtained structures are at the local

TABLE 2: Structural Parameters and Atomic Charge of the Ag(I) Ion Solvated with Hydrogen Cyanide and Acetonitrile

n	point group	Ag−N/pm	N−C/pm	C−H or C−C/pm	atomic charge on Ag	total energy/au
			HCN-Solvated Ag(I) Ions			
0					1.0000	−5193.420 334
1	$C_{\infty v}$	238	113	108	0.8967	−5286.233 950
2	$D_{\infty h}$	238	113	108	0.8083	−5379.042 627
3	D_{3h}	247	113	107	0.7582	−5471.839 904
4	T_d	254	113	107	0.7244	−5564.630 627
5[a]	D_{3h}	267 261	113 113	107 107	0.7130	−5657.412 908
6	O_h	271	113	107	0.6901	−5750.192 579
isolated[b]	$C_{\infty v}$		113	107		−92.769 619
			CH_3CN-Solvated Ag(I) Ions			
0					1.0000	−5193.420 334
1	C_{3v}	236	113	145	0.8951	−5325.139 425
2	D_{3d}	236	113	145	0.8097	−5456.853 105
3	D_{3h}	245	113	145	0.7627	−5588.553 912
4	T_d	253	113	145	0.7332	−5720.248 019
5[a]	D_{3h}	266 260	113 113	145 145	0.7277	−5851.933 403
isolated[b]	C_{3v}		113	145		−131.673 228

[a] There are equatorial and axial positions in the pentacoordinated trigonal bipyramidal structure. Figures in the upper and lower columns correspond to lengths of the axial and equatorial bonds, respectively. [b] “Isolated” means isolated HCN or CH_3CN molecules.

TABLE 3: Thermodynamic Parameters of Gas Phase Reactions, $Ag^+ + n$HCN → $[Ag(NCH)_n]^+$ (n = 1−6) and $Ag^+ + nCH_3CN$ → $[Ag(NCCH_3)_n]^+$ (n = 1−5), at 1 atm and 25.0 °C[a]

		internal energy (U)				entropy (S)			
n	$-\Delta E_{solv}$	reactant	product	$-\Delta U$	$-\Delta H$	reactant	product	$-\Delta S$	$-\Delta G_{solv}$
			$Ag^+ + n$HCN → $[Ag(NCH)_n]^+$ (n = 1−6)						
1	25.5	13.6	14.6	24.5	25.1	87.8	65.5	22.3	18.4
2	48.1	26.2	29.0	45.4	46.6	135.7	88.1	47.6	32.4
3	64.0	38.9	42.9	60.1	61.8	183.6	111.6	72.0	40.4
4	76.0	51.6	57.1	70.5	72.9	231.5	135.5	95.9	44.3
5	83.3	64.3	71.3	76.4	79.3	279.3	162.4	116.9	44.5
6	88.9	77.0	85.4	80.5	84.0	327.2	186.8	140.4	42.2
			$Ag^+ + nCH_3CN$ → $[Ag(NCCH_3)_n]^+$ (n = 1−5)						
1	26.4	31.7	32.4	25.7	26.3	97.8	75.4	22.5	19.6
2	49.6	62.4	64.6	47.4	48.6	155.6	107.1	48.5	34.1
3	65.3	93.2	96.6	62.0	63.8	213.5	144.5	69.0	43.2
4	77.0	124.0	128.8	72.2	74.6	271.4	174.9	96.4	45.8
5	83.8	154.8	161.1	77.5	80.5	329.2	213.3	116.0	45.9

[a] The unit is kcal mol^{-1} except for entropy (S) (cal mol^{-1} K^{-1}). U contains zero-point vibrational energy. $\Delta U = \Delta E_{solv} + [U(\text{product}) - U(\text{reactant})]$. H means enthalpy.

minima on the potential surface. As is apparent from figures in Table 2, the bond lengths of N−C, C−H, and C−C in the solvated silver(I) species are not affected by the coordination number, while the species have the variation in both the Ag−N bond length and the charge on the silver atom. There is a trend that the positive charge on the Ag(I) cation decreases with increasing the solvation number until 4 and becomes flat over 4 for both HCN- and CH_3CN-solvated Ag(I) ions. The donation of electrons from the coordinated solvent molecules enables the central cation to disperse its positive charge. The occurrence of sp, sp^2 or sp^3 hybridization among unoccupied 5s and 5p efficiently helps the charge dispersion in the case of the solvation number lower than 5, and the stabilization by such a dispersion process does not much occur for the solvation number of more than 4.

In Table 3 are listed the thermodynamic parameters for solvation of the silver(I) ion with HCN and CH_3CN at 1 atm and 25 °C. The degree of decrease in ΔE_{solv} decreases with an increase in the solvation number that corresponds to the trend of decrease in the atomic charge on Ag. It should be noted that ΔE_{solv} contains the contribution of the van der Waals repulsion between coordinated solvent molecules. Figure 4 shows the variation of ΔH, ΔS, and ΔG_{solv} as a function of coordination number. The value of ΔS monotonously decreases with increasing the coordination number. The contribution of the entropy, thus, overcomes that of ΔH in the coordination number over 4. The stabilization energies given with ΔG_{solv} in the last column in Table 3 become maximal at n = 4 or 5 for both solvents.

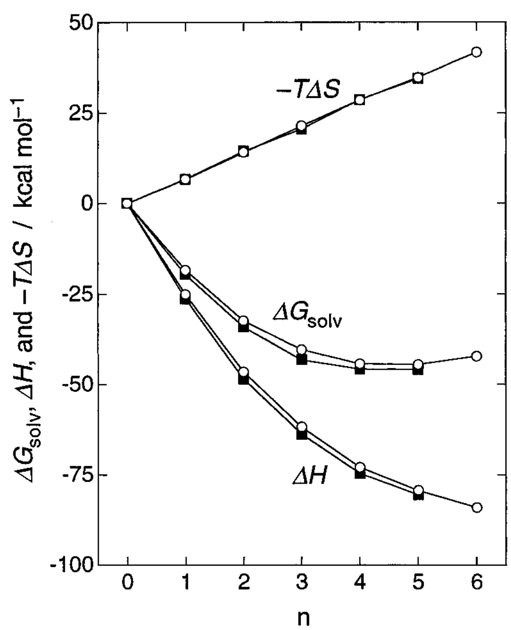

Figure 4. Variation of ΔH, ΔS, and ΔG_{solv} as a function of n at 1 atm and 25 °C. Circles represent HCN, and squares represent CH_3CN.

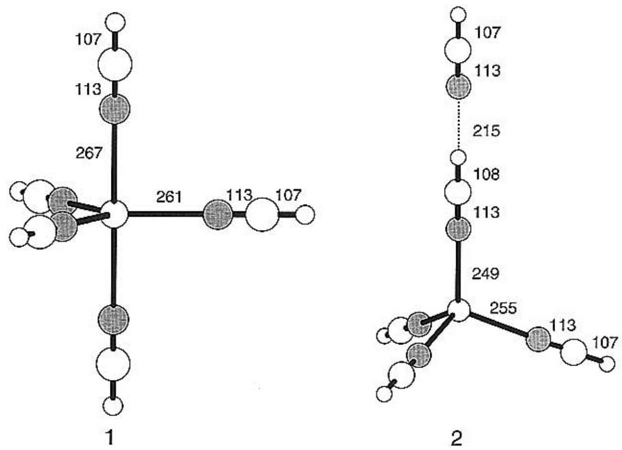

Figure 5. Structure of products (**1** and **2**) in reactions 5 and 6.

In order to an energetic comparison of solvation with $n = 4$ and 5, it is valuable to compare reactions 5 and 6. Figure 5 shows the structures of the products in reactions 5 and 6 that are at the local minima. For reactions 5 and 6, the ΔE_{solv} values have been calculated to be -83.3 and -84.8 kcal mol^{-1}, respectively, and the values of ΔG_{solv} are -44.5 and -46.4 kcal mol^{-1}, respectively. Thus, the value of ΔG_{solv} for reaction 6 is smaller than that for reaction 5. Therefore, the fifth solvent molecule prefers occupying the outer coordination sphere to occupying the first-coordination sphere. The structure of **2** in Figure 5 shows that the coordinated hydrogen cyanide interacted with one in the outer sphere has a shorter Ag−N distance (249 pm) by 6 pm than the other coordinated hydrogen cyanides without such an interaction. This fact indicates that HCN molecules in the outer sphere should polarize them in the first-coordination sphere and such an effect results in the enhancement of donation of the coordinated HCN molecules. Such an enhancement in the HCN system can also be expected in the CH_3CN system. Consequently, the solvation number of the Ag(I) ion is 4, which is consistent with the results of the experimental observations in solution.

In conclusion, the solvation number of 4 for the silver(I) ion in 10 neat solvents in this work is interpreted by the balance between ΔE_{solv} and ΔS contribution to ΔG_{solv}. The relatively smaller electronic stabilizations for solvation of the Ag(I) ion with a lower charge, a larger ionic radius, and d^{10} electronic configuration are compensated by the ΔS and the van der Waals repulsion between bound solvent molecules.

Acknowledgment. This work was supported by Grants-in-Aid for Scientific Research (Nos. 0745199 and 07504003) from the Ministry of Education, Science, Sports, and Culture of Japan. The EXAFS measurements were performed under the approval of the Photon Factory Program Adversary Committee (Proposal No. 94G003).

References and Notes

(1) (a) Nagoya University. (b) Gifu University.
(2) Nilsson, K.; Oskarsson, Å. *Acta Chem. Scand.* **1984**, *A38*, 79.
(3) Nilsson, K.; Oskarsson, Å. *Acta Chem. Scand.* **1982**, *A36*, 605.
(4) Dyason, J. C.; Healy, P. C.; Engelhardt, L. M.; White, A. H. *Aust. J. Chem.* **1985**, *38*, 1325.
(5) Goodwin, K. V.; McMillin, D. R.; Robinson, W. R. *Inorg. Chem.* **1986**, *25*, 2033.
(6) Yamaguchi, T.; Lindqvist, O. *Acta Chem. Scand.* **1983**, *A37*, 685.
(7) Antti, C.-J.; Lundberg, B. K. S. *Acta Chem. Scand.* **1971**, *25*, 1758.
(8) Bjerrum, J. *Acta Chem. Scand.* **1986**, *A40*, 392.
(9) Carlucci, L.; Ciani, G.; Proserpio, D. M.; Sironi, A. *J. Am. Chem. Soc.* **1995**, *117*, 4562.
(10) Richmond, T. G.; Kelson, E. P.; Arif, A. M. *J. Am. Chem. Soc.* **1988**, *110*, 2334.
(11) Richmond, T. G.; Kelson, E. P.; Patton, A. T. *J. Chem. Soc., Chem. Commun.* **1988**, 96.
(12) Yamaguchi, T.; Lindqvist, O.; Boyce, J. B.; Claeson, T. *Acta Chem. Scand.* **1984**, *A38*, 423.
(13) Sandström, M.; Nielson, G. W.; Johansson, G.; Yamaguchi, T. *J. Phys. C: Solid State Phys.* **1985**, *18*, L1115.
(14) Yamaguchi, T.; Johansson, G.; Holmberg, B.; Maeda, M.; Ohtaki, H. *Acta Chem. Scand.* **1984**, *A38*, 437.
(15) Maeda, M.; Maegawa, Y.; Yamaguchi, T.; Ohtaki, H. *Bull. Chem. Soc. Jpn.* **1979**, *52*, 2545.
(16) Yamaguchi, T.; Wakita, H.; Nomura, M. *J. Chem. Soc., Chem. Commun.* **1988**, 433.
(17) Hultén, F.; Persson, I. *Acta Chem. Scand.* **1987**, *A41*, 87.
(18) Nilsson, K.; Persson, I. *Acta Chem. Scand.* **1987**, *A41*, 139.
(19) Inada, Y.; Sugimoto, K.; Ozutsumi, K.; Funahashi, S. *Inorg. Chem.* **1994**, *33*, 1875.
(20) Shannon, R. D. *Acta Crystallogr.* **1976**, *A32*, 751.
(21) Soyama, S.; Ishii, M.; Funahashi, S.; Tanaka, M. *Inorg. Chem.* **1992**, *31*, 536.
(22) Nomura, M. *KEK Report 85-7*; National Laboratory for High Energy Physics: Tsukuba, Japan, 1985.
(23) Nomura, M.; Koyama, A. *KEK Report 89-16*; National Laboratory for High Energy Physics: Tsukuba, Japan, 1989.
(24) Sayers, D. E.; Stern, E. A.; Lytle, F. W. *Phys. Rev. Lett.* **1971**, *27*, 1204.
(25) Stern, E. A. *Phys. Rev. B* **1974**, *10*, 3027.
(26) Stern, E. A.; Sayers, D. E.; Lytle, F. W. *Phys. Rev. B* **1975**, *11*, 4836.
(27) Lengeler, B.; Eisenberger, P. *Phys. Rev. B* **1980**, *21*, 4507.
(28) McKale, A. G.; Veal, B. W.; Paulikas, A. P.; Chan, S. K.; Knapp, G. S. *J. Am. Chem. Soc.* **1988**, *110*, 3763.
(29) Huzinaga, S. *Physical Science Data 16, Gaussian Basis Sets for Molecular Calculations*; Elsevier: New York, 1984.
(30) Boys, S. F.; Bernardi, F. *Mol. Phys.* **1970**, *19*, 553.
(31) ΔE_{BSSE} of reaction 2 or 3 is given by $\Delta E_{BSSE} = (E(Ag^+) + E(\text{solvents})) - (E(Ag^+,G) + E(\text{solvents},G))$, where E means the total energy of species and solvents and G in parentheses represents solvents keeping an appropriate coordination structure and ghost orbitals, respectively.
(32) Knox, J. H. *Molecular Thermodynamics. An Introduction to Statistical Mechanics for Chemists*; John-Wiley & Sons: New York, 1971.
(33) Reaction 6 is divided into two-step reactions in order to calculate BSSE.

$$Ag^+ + 4HCN \rightarrow [Ag(NCH)_4]^+ \quad (6a)$$

$$[Ag(NCH)_4]^+ + HCN \rightarrow [Ag(NCH)_4]^+\cdot NCH \quad (6b)$$

Here, the geometry of $[Ag(NCH_4)]^+$ corresponds to the partial structure of the optimized $[Ag(NCH_4)]^+\cdot NCH$ complex. The BSSE of reactions 6a and 6b is given by the following equation.

$$\Delta E_{BSSE} = \{(E(Ag^+) + E((HCN)_4)) - (E(Ag^+,G) + E((HCN)_4,G))\} + \{(E([Ag(NCH)_4]^+) + E(HCN)) - (E([Ag(NCH)_4]^+,G) + E(HCN,G))\}$$

(34) Frisch, M. J.; Trucks, G. W.; H.-Gordon, M.; Gill, P. M. W.; Wong, M. W.; Foresman, J. B.; Johnson, B. G.; Schlegel, H. B.; Robb, M. A.; Replogle, E. S.; Gomperts, R.; Andres, J. L.; Raghavachari, K.; Binkley, J. S.; Gonzalez, C.; Martin, R. L.; Fox, D. J.; Defrees, D. J.; Baker, J.; Stewart, J. J. P.; Pople, J. A. *Gaussian 92 Revision C*; Gaussian, Inc.: Pittsburgh, PA, 1992.
(35) Tsutsui, Y.; Wasada, H. *Chem. Lett.* **1995**, 517.
(36) Chang, T.-C. G.; Irish, D. E. *J. Solution Chem.* **1974**, *3*, 175.
(37) Melanson, R.; Rochon, F. D. *Can. J. Chem.* **1975**, *53*, 2371.
(38) Bennett, M. J.; Cotton, F. A.; Weaver, D. L.; Williams, R. J.; Watson, W. H. *Acta Crystallogr.* **1967**, *23*, 788.
(39) Rochon, F. D.; Kong, P. C.; Melanson, R. *Can. J. Chem.* **1983**, *61*, 1823.
(40) Sandström, M.; Persson, I. *Acta Chem. Scand.* **1978**, *A32*, 95.
(41) Sandström, M. *Acta Chem. Scand.* **1978**, *A32*, 519.
(42) Elding, L. I.; Oskarsson, Å. *Inorg. Chim. Acta* **1987**, *130*, 209.
(43) Mercer, A.; Trotter, J. *J. Chem. Soc., Dalton Trans.* **1975**, 2480.
(44) Persson, I.; P.-Hahn, J. E.; Hodgson, K. O. *Inorg. Chem.* **1993**, *32*, 2497.
(45) Inada, Y.; Ozutsumi, K.; Funahashi, S.; Soyama, S.; Kawashima, T.; Tanaka, M. *Inorg. Chem.* **1993**, *32*, 3010.
(46) Bang, E. *Acta Chem. Scand.* **1978**, *A32*, 555.
(47) Johnsson, M.; Persson, I. *Inorg. Chim. Acta* **1987**, *127*, 35.
(48) Fleming, J. E.; Lynton, H. *Can. J. Chem.* **1968**, *46*, 471.
(49) Deloume, J.-P.; Faure, R.; Loiseleur, H. *Acta Crystallogr.* **1977**, *B33*, 2709.